

# PyFLOSIC - Python based Fermi-Löwdin orbital self-interaction correction

Sebastian Schwalbe<sup>a,\*</sup>, Lenz Fiedler<sup>a,b</sup>, Torsten Hahn<sup>a</sup>, Kai Trepte<sup>c</sup>, Jakob Kraus<sup>a</sup>, Jens Kortus<sup>a</sup>

<sup>a</sup>*Institute of Theoretical Physics, TU Bergakademie Freiberg, Leipziger Str. 23, D-09596 Freiberg, Germany*

<sup>b</sup>*Freiberg Instruments GmbH, Delfter Str.6, D-09599 Freiberg, Germany*

<sup>c</sup>*Department of Physics, Central Michigan University, Mount Pleasant, MI 48859, USA*

---

## Abstract

The Fermi-Löwdin orbital self-interaction correction (FLO-SIC) method addresses the self-interaction error within density functional theory (DFT). We present PyFLOSIC, an open-source python implementation of FLO-SIC that is based on the highly modular and modern PySCF electronic structure code. This implementation offers the possibility to use FLO-SIC with any kind of basis set (e.g from the EMSL data base), different numerical meshes (e.g. Lebedev-Laikov grids) and any exchange-correlation functional available in the libxc library. The FLO-SIC method relies on so-called Fermi-orbital descriptors (FODs). We provide a generator for starting values of these FODs which is based on centers of mass of localized orbitals (PyCOM). For the optimization of the FODs, a calculator and an optimizer class for the atomic simulation environment (ase) are included. We present several proof-of-principles calculations and extensive benchmarks against the reference FLO-SIC implementation. The thermochemical performance and ionization potentials of FLO-SIC for the G2-1 benchmark set are analyzed using the local spin density approximation (LSDA), the Perdew-Burke-Ernzerhof (PBE) and the strongly-constrained and appropriately-normed (SCAN) functional.

*Keywords:* electronic structure; density functional theory; FLO-SIC; Unified Hamiltonian; SCAN

---

\*Corresponding author.

*E-mail address:* schwalbe@physik.tu-freiberg.de

## PROGRAM SUMMARY

*Manuscript Title: PyFLOSIC - Python based Fermi-Löwdin orbital self-interaction correction*

*Authors: S. Schwalbe, L. Fiedler, T. Hahn, K. Trepte, J. Kortus*

*Program Title: PyFLOSIC*

*Programming language: Python3*

*Computer: Tested on several Linux distributions (Debian, Ubuntu, OpenSuse, Scientific Linux etc.) and Mac OS. The code is written in Python3.*

*Operating system: Unix/Linux*

*Keywords: electronic structure, density functional theory, FLO-SIC, Unified Hamiltonian, SCAN*

*External routines/libraries: pycsf (1.6.1), h5py (2.9.0), numpy (1.16.3), scipy (1.2.1), libxc (4.X or higher), ase (3.17.0)*

*Nature of problem:* The method is addressing the self-interaction error within density functional theory (DFT) [1], an error of density functional approximations that leads to several shortcomings in DFT.

*Solution method:* We offer a new implementation of the Fermi-Löwdin orbital self-interaction correction (FLO-SIC) [2] applicable to any functional within the libxc library [3]. Our python code is based on the PySCF infrastructure [4] and is written in a user-friendly way, designed for easy and fast code development.

*Unusual features:* PyFLOSIC has an subroutine for the automatic generation of Fermi-orbital descriptors (PyCOM).

- [1] Self-interaction correction to density-functional approximations for many-electron systems, Perdew, J. P. and Zunger, A., Phys. Rev. B, 23, 10, 5048, 1981, APS
- [2] Communication: Self-interaction correction with unitary invariance in density functional theory, Pederson, M. R. and Ruzsinszky, A. and Perdew, J. P., J. Chem. Phys., 140, 121103, 2014, AIP
- [3] Recent developments in libxc-A comprehensive library of functionals for density functional theory, Lehtola, S. and Steigemann, C. and Oliveira, M. J. T. and Marques, M. A. L., SoftwareX, 7, 1-5, 2018, Elsevier
- [4] PySCF: the Python-based simulations of chemistry framework, Sun, Q. and Berkelbach, T. C. and Blunt, N. S. and Booth, G. H. and Guo, S. and Li, Z. and Liu, J. and McClain, J. D. and Sayfutyarova, E. R. and Sharma, S. and others, Wiley Interdiscip. Rev. Comput. Mol. Sci., 8, 1, 2018, e1340, Wiley Online Library

## 1. Introduction

Density functional theory (DFT) [1, 2] has become one of the standard methods in computational materials science, condensed matter physics and chemistry based on its reasonable accuracy and computational efficiency [3, 4]. However, DFT is known to fail for properties like ionization potentials calculated from the energy of the highest occupied orbital (HOMO)  $IP = -\epsilon_{\text{HOMO}}$  or stretched-bond situations [5]. Another problem is the correct description of negatively charged species. In such situations, a self-interaction correction (SIC) applied on-top of DFT may reduce errors of the pure functionals significantly [6].

John Perdew established the so-called "Jacob's ladder" for DFT [7], which classifies the ability of a certain rung of exchange-correlation functionals to achieve chemical accuracy. In this work, we selected one functional of the lowest rung the local density approximation (LDA), LDA-PW91 [8], one of the second rung of the generalized-gradient approximations (GGAs), GGA-PBE [9], and one from the third rung of meta-GGAs, MGGA-SCAN [10]. The performance of the pure functional and the respective Fermi-Löwdin orbital self-interaction correction (FLO-SIC) [11–15] functional for several benchmarks including the thermochemical performance for the G2-1 benchmark set are discussed [6]. This paper presents the first systematic SCAN-FLO-SIC results for several different benchmarks.

Our implementation of the FLO-SIC method (FLO-SIC) is based on the PySCF [16] electronic structure code. However, the implementation presents a strategy viable for any Gaussian-type orbital (GTO) [17] electronic structure code. We will discuss similarities and differences to the original FLO-SIC implementation by Pederson and co-workers [6, 11, 13, 18–20] in detail. The PyFLOSIC code and related software (e.g. additional FOD generators) are available on github at the PyFLOSIC organization (<https://github.com/pyflosic>).

In section Theoretical Background, the strategy for the implementation of FLO-SIC in the PySCF [16] code is presented, and in section Workflow, we discuss numerical details. Afterwards, FLO-SIC results using the local spin density approximation (LSDA; shorthand LDA) [8], the Perdew-Burke-Ernzerhof (PBE) [9] and the strongly-constrained and appropriately-normed (SCAN) [10] functional are discussed, followed by an outlook.

## 2. Theoretical Background

We adopted the notation introduced by Lehtola and Jónsson [21]. Vectors are expressed in bold, non-italic letters ( $\mathbf{a}$ ) and matrices are given in bold, italic letters ( $\mathbf{R}$ ). We express the FLO-SIC method in terms of the density matrix formalism. If not stated otherwise, atomic units are used for the derivation and throughout this paper.

### 2.1. Hamiltonian and self-consistent cycle

The total energy in the Kohn-Sham (KS) DFT formalism is given by

$$E_{\text{KS}}[n] = T_s[n] + V[n] + J[n] + K[n], \quad (1)$$

with  $E_{\text{KS}}[n]$  the total KS energy,  $T_s[n]$  the kinetic energy of the non-interacting system,  $V[n]$  the external potential energy,  $J[n]$  the Coulomb energy and  $K[n]$  the exchange-correlation energy. The SIC energy can be defined using [22]

$$E_{\text{SIC}} = E_{\text{KS}}[n^\alpha, n^\beta] - \sum_{i\sigma} (K[n_i^\sigma, 0] + J[n_i^\sigma]), \quad (2)$$

with  $\sigma$  denoting the spin being either  $\alpha$  or  $\beta$  and  $n_i^\sigma$  being single-orbital densities. For standard DFT, one can perform the self-consistent field calculation (iterative procedure often used in computational quantum chemistry and physics) using

$$\mathbf{F}_{\text{KS}}^\sigma = \mathbf{H}_{\text{core}} + \mathbf{J} + \mathbf{K}^\sigma, \quad (3)$$

where  $\mathbf{H}_{\text{core}}$  is

$$\mathbf{H}_{\text{core}} = -\frac{1}{2}\nabla^2 - \sum_A^{\text{nuclei}} \frac{Z_A}{|\mathbf{r} - \mathbf{r}_A|}, \quad (4)$$

with  $\nabla$  being the Nabla operator and  $Z_A$  being the nuclear charge of atom  $A$  at position  $\mathbf{r}_A$ . The SIC Hamiltonian is similar to the Pople-Nesbet-Roothaan-Hall type [23, 24] and can be written as

$$(\mathbf{F}_{\text{KS}}^\sigma + \mathbf{F}_{\text{SIC}}^\sigma)\mathbf{C}^\sigma = \mathbf{S}\mathbf{C}^\sigma\mathbf{E}^\sigma, \quad (5)$$

with  $\mathbf{C}^\sigma$  being a matrix containing the KS molecular orbital coefficients,  $\mathbf{S}$  is the overlap matrix and  $\mathbf{E}^\sigma$  is a diagonal matrix holding the energy eigenvalues. The SIC Hamiltonian can be derived from the unified Hamiltonian (see Harrison et al. [25] and see Lehtola and Jónsson [21] Eq. (37))

$$\mathbf{F}_{\text{SIC}}^\sigma = -\frac{1}{2} \sum_{i=1}^{N^\sigma} (\mathbf{f}_i^\sigma \mathbf{p}_i^\sigma \mathbf{S} + \mathbf{S} \mathbf{p}_i^\sigma \mathbf{f}_i^\sigma). \quad (6)$$

This form of the Hamiltonian effectively treats only the occupied-occupied (OO) space and ignores the occupied-virtual (OV) space. In this context,  $\mathbf{f}_i = \mathbf{J}(\mathbf{p}_i^\sigma) + \mathbf{K}(\mathbf{p}_i^\sigma)$  is the KS-Fock matrix of the  $i$ -th density matrix  $\mathbf{p}_i^\sigma$  given by

$$\mathbf{p}_i^\sigma = \mathbf{c}_i^\sigma \mathbf{c}_i^{\sigma\dagger}, \quad (7)$$

with  $\mathbf{c}_i^\sigma$  being the  $i$ -th column of the FLO molecular orbital coefficient matrix, containing the coefficients of FLO  $\phi_i$ .

## 2.2. Localized orbitals

Using a Gaussian-type orbital basis, the Kohn-Sham wavefunctions  $\psi_\alpha$  can be expressed as

$$\psi_\alpha = \sum_s c_\alpha^s f^s, \quad (8)$$

with  $s$  being the running index of all basis functions  $f^s$  with the corresponding coefficients  $c_\alpha^s$ . Within FLO-SIC, so-called Fermi orbitals (FO,  $|FO_i\rangle$ ) are constructed from the original Kohn-Sham wavefunctions  $\psi_\alpha$  via

$$|FO_i\rangle = \sum_{\alpha=1}^N R_{i\alpha} |\psi_\alpha\rangle, \quad (9)$$

where the transformation matrix  $\mathbf{R}$  is defined as

$$R_{i\alpha} = \frac{\psi_\alpha^*(\mathbf{a}_i)}{\sqrt{\sum_{\alpha=1}^N |\psi_\alpha(\mathbf{a}_i)|^2}}. \quad (10)$$

The  $\mathbf{a}_i$  are points in real space called Fermi-orbital descriptors (FODs). The knowledge of these FODs is necessary for the construction of the Fermi orbitals.

To simplify notation, we express both the Fermi orbitals and the Kohn-Sham orbitals as vectors containing the actual orbitals. For  $N$  electrons, these vectors will contain  $N$  elements. The Kohn-Sham orbitals and Fermi orbitals, respectively, therefore read

$$\boldsymbol{\Psi} = (|\psi_1\rangle, |\psi_2\rangle, \dots, |\psi_N\rangle)^\dagger, \quad (11)$$

$$\mathbf{FO} = (|FO_1\rangle, |FO_2\rangle, \dots, |FO_N\rangle)^\dagger, \quad (12)$$

and Eq. (10) can be expressed simply as

$$\mathbf{FO} = \mathbf{R}\boldsymbol{\psi} . \quad (13)$$

Another technical issue should be noted here. It is common to use non-orthonormal basis sets, e.g. non-orthonormal linear combinations of atom-centered functions. When using orthonormal basis sets, the atomic overlap matrix  $\mathbf{S}_{1e}$  of the atomic basis functions is simply the unit matrix  $\mathbb{1}$ , and we obtain

$$\boldsymbol{\psi}^\dagger \mathbf{S}_{1e} \boldsymbol{\psi} = \mathbb{1} . \quad (14)$$

Please note that Fermi orbitals given by Eq. (13) generally do not satisfy Eq. (14), i.e.

$$\mathbf{FO}^\dagger \mathbf{S}_{1e} \mathbf{FO} = \mathbf{S} \neq \mathbb{1} , \quad (15)$$

introducing the overlap matrix  $\mathbf{S}$ . Therefore, to obtain an orthogonal set of localized orbitals, a symmetric Löwdin orthogonalization [26] is carried out. This can be achieved by solving the corresponding eigenvalue problem for the overlap matrix  $\mathbf{S}$

$$\mathbf{S}\mathbf{T}_\alpha = Q_\alpha \mathbf{T}_\alpha , \quad (16)$$

with the eigenvectors  $\mathbf{T}_\alpha$  and the eigenvalues  $Q_\alpha$ . With these, one can transform the Fermi orbitals  $\mathbf{FO}$  into Fermi-Löwdin orbitals  $\boldsymbol{\phi}$  by

$$\boldsymbol{\phi} = \mathbf{T}\mathbf{Q}^{-1/2}\mathbf{T}^\dagger\mathbf{FO} . \quad (17)$$

Here, the matrix  $\mathbf{T}$  is defined as the matrix of the eigenvectors, while  $\mathbf{Q}^{-1/2}$  is

$$Q_{ij}^{-1/2} = \begin{cases} Q_i^{-1/2} & , i = j \\ 0 & , i \neq j . \end{cases} \quad (18)$$

The resulting Fermi-Löwdin orbitals  $\boldsymbol{\phi}$  now satisfy Eq. (14), i.e.

$$\boldsymbol{\phi}^\dagger \mathbf{S}_{1e} \boldsymbol{\phi} = \mathbb{1} . \quad (19)$$

The complete transformation from Kohn-Sham to Fermi-Löwdin orbitals

$$\boldsymbol{\phi} = \mathbf{T}\mathbf{Q}^{-1/2}\mathbf{T}^\dagger\mathbf{R}\boldsymbol{\psi} \quad (20)$$

is unitary, leaving the density unchanged. The constructed Fermi-Löwdin orbitals can now be used to perform the self-interaction correction.

### 2.3. Implementation specifics

Our PyFLOSIC code has been intensively benchmarked against the reference implementation in FG-NRLMOL. FG-NRLMOL is a highly optimized developer version of the NRLMOL code [27–33]. In our implementation, we make use of the unified Hamiltonian formalism [21] instead of the Pederson SIC Hamiltonian [13].

Moreover, the exchange-correlation potentials are not explicitly calculated on a numerical grid  $V_{xc}(\mathbf{r})$ . Instead, we are using a density matrix formalism delivering potential matrices  $\mathbf{V}_{xc}$ . This allows us to apply our method to any functional in the libxc library [34]. The differences to the reference implementation in our FG-NRLMOL code are highlighted in Tab. 1.

Table 1: Implementation differences.

<b>FG-NRLMOL</b>	<b>PyFLOSIC</b>
$V_{xc}(\mathbf{r})$	$\mathbf{V}_{xc}$
$\boldsymbol{\psi}^\dagger \boldsymbol{\psi} = \mathbb{1}$	$\boldsymbol{\psi}^\dagger \mathbf{S}_{1e} \boldsymbol{\psi} = \mathbb{1}$
Pederson Hamiltonian [13]	Unified Hamiltonian [25]

### 3. Workflow

We implemented the FLO-SIC method using the PySCF code [16] for the DFT part. Core routines were developed during the master thesis of Lenz Fiedler [35]. The modern PySCF open-source electronic structure code includes many standard libraries (e.g. libxc library for exchange and correlation functionals, libcint library [36] for Gaussian-type orbital integral handling). Therefore, FLO-SIC can be combined with any exchange-correlation functional in the libxc library. Furthermore, PySCF offers a variety of functionalities from Hartree-Fock (HF) to CCSD(T) theory, enabling a direct comparison of FLO-SIC results with results from quantum chemical methods.

The density matrix formalism has been used successfully to implement self-interaction correction before, namely in the ERKALE code [21], which also offers access to the libxc library. The PyFLOSIC implementation is, just like ERKALE, based on density matrices. We took advantage of routines and architecture provided by PySCF as much as possible (see Fig. 1 as well).

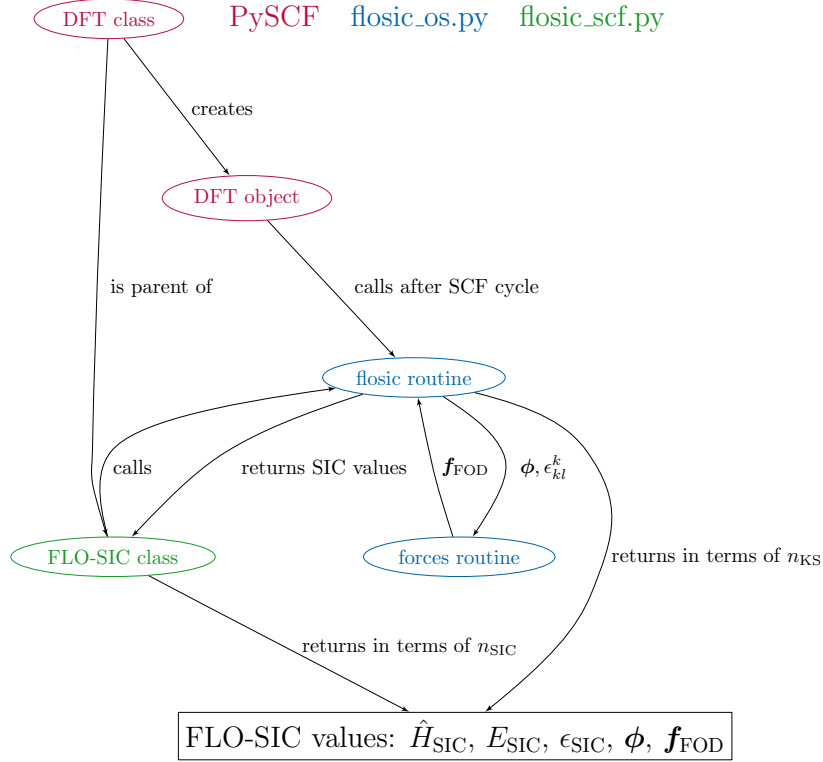


Figure 1: PyFLOSIC chart.

PyFLOSIC is currently OpenMP parallelized and contains MPI functionality for numerically expensive parts.

There are two options to perform FLO-SIC calculations. First, a one-shot (FLO-SIC-OS) mode as a post-processing option. The FLO-SIC-OS mode keeps the density of the underlying DFT calculations. The second option is a fully variational self-consistent FLO-SIC (FLO-SIC-SCF) mode. The FLO-SIC-SCF mode updates the self-interaction corrected density during the self-consistent field calculation. The FLO-SIC self-consistent field cycle is summarized in Fig. 2. We have implemented two unified Hamiltonians [25]. The first one only treats the occupied-occupied (OO) space

$$\mathbf{F}_{\text{OO}}^{\text{SIC}} = -\frac{1}{2} \sum_{i=1}^{N^\sigma} (\mathbf{f}_i^\sigma \mathbf{p}_i^\sigma \mathbf{S} + \mathbf{S} \mathbf{p}_i^\sigma \mathbf{f}_i^\sigma), \quad (21)$$



whereas the second one additionally includes the occupied-virtual (OV) space

$$\mathbf{F}_{\text{OO,OV}}^{\text{SIC}} = -\mathbf{S} \sum_{i=1}^{N^\sigma} (\mathbf{p}_i^\sigma \mathbf{f}_i^\sigma \mathbf{p}_i^\sigma + \mathbf{v}^\sigma \mathbf{f}_i^\sigma \mathbf{p}_i^\sigma + \mathbf{p}_i^\sigma \mathbf{f}_i^\sigma \mathbf{v}^\sigma) \mathbf{S}. \quad (22)$$

Here, we introduced the virtual space projector

$$\mathbf{v}^\sigma = \sum_i^{\text{virtual}} \mathbf{C}_i^\sigma \mathbf{C}_i^{\sigma\dagger}, \quad (23)$$

with  $\mathbf{C}_i^\sigma$  being the  $i$ -th column of  $\mathbf{C}^\sigma$ . As a guide for the eyes, please see the Hamiltonian written as a matrix

$$\mathbf{F}^{\text{SIC}} = \begin{pmatrix} \mathbf{F}_{\text{OO}} & \mathbf{F}_{\text{OV}} \\ \mathbf{F}_{\text{VO}} & \mathbf{F}_{\text{VV}} \end{pmatrix} = \begin{pmatrix} \mathbf{F}_{\text{OO}} & \mathbf{F}_{\text{OV}} \\ \mathbf{F}_{\text{VO}} & 0 \end{pmatrix} \quad (24)$$

Lehtola provides a good overview for unified Hamiltonians [21]. The different unified Hamiltonians can be used in the PZ-SIC implementation within Lehtola’s ERKALE code[37]. The  $\mathbf{F}_{\text{OO}}^{\text{SIC}}$  was used for all values presented here. While in FLO-SIC-OS mode the projectors are not updated, in the FLO-SIC-SCF mode they are updated in a variational self-consistent fashion. Regarding that and using the full unified Hamiltonian  $H_{\text{OOOV}}$ , we obtain identical results compared to the variational method proposed by Pederson[13]. A detailed comparison between different SIC Hamiltonians will be published elsewhere.

In FLO-SIC, the total energy including the self-interaction energy depends on the FODs. In order to find the minimum of the energy, the FODs need to be optimized. Each FOD is a point in three-dimensional space. The collection of all FODs forms the so-called electronic geometry of the system, in analogy to the molecular geometry formed by all nuclei positions.

Each FLO-SIC calculation starts from an initial set of FODs. PyFLOSIC comes with the python center of mass (PyCOM) module, which allows to obtain such initial FOD positions. The numerical cost is that of a standard DFT calculation plus the cost of the localization of Kohn-Sham orbitals using Foster-Boys, Edmiston-Ruedenberg or Pipek-Mezey localization procedures [38] for each spin channel. Alternative approaches for the automatic generation of FODs are discussed elsewhere by Schwalbe et al. [39].

The initial set of FODs can be optimized with different non-linear optimization algorithms such as conjugate gradient, L-BFGS [40–44] or the FIRE

algorithm [45]. Interfaces to the atomic simulation environment (ase) [46, 47] are also provided, allowing to access the optimization algorithms implemented there.

If a FOD optimization is performed, the FOD geometry is optimized until the forces on the FOD geometry obey a convergence criterion of  $F_{\max} \leq 5 \cdot 10^{-3} E_h/a_0$ . PySCF offers many standard basis sets (e.g. Pople basis sets like 6-311G or Dunning’s correlation consistent basis sets like cc-pvqz). In addition, we formatted the NRLMOL density functional optimized (DFO) [48] basis set to Gaussian94 basis set (gbs) format. This allows the usage of this basis set with PySCF.

## 4. Code features

The PyFLOSIC code offers the following features:

- one-shot (os; fixed DFT density) and self-consistent field (scf; FLO-SIC optimized density) modes
- automatic FOD guessing procedure
  - e.g. PyCOM - Python Center Of Mass
- visualization of FLOs and densities
- analytic FOD forces
- various FOD optimization procedures
  - e.g. CG, (L-)BFGS, FIRE etc.
- as few input parameters as possible
  - calculation script and geometry file
- transparent usage of all PySCF features
  - e.g. Newton-Raphson SCF cycle or density fitting procedures
- Gaussian type basis sets
  - all-electron and effective core potential
- all  $E_{XC}$  functionals from libxc
  - e.g. LDA-PW, PBE and SCAN

## 5. Input files

### 5.1. Geometry input file

As for any electronic structure calculation, one needs an input file for the nuclei species and their positions. In PyFLOSIC, we start from a standard

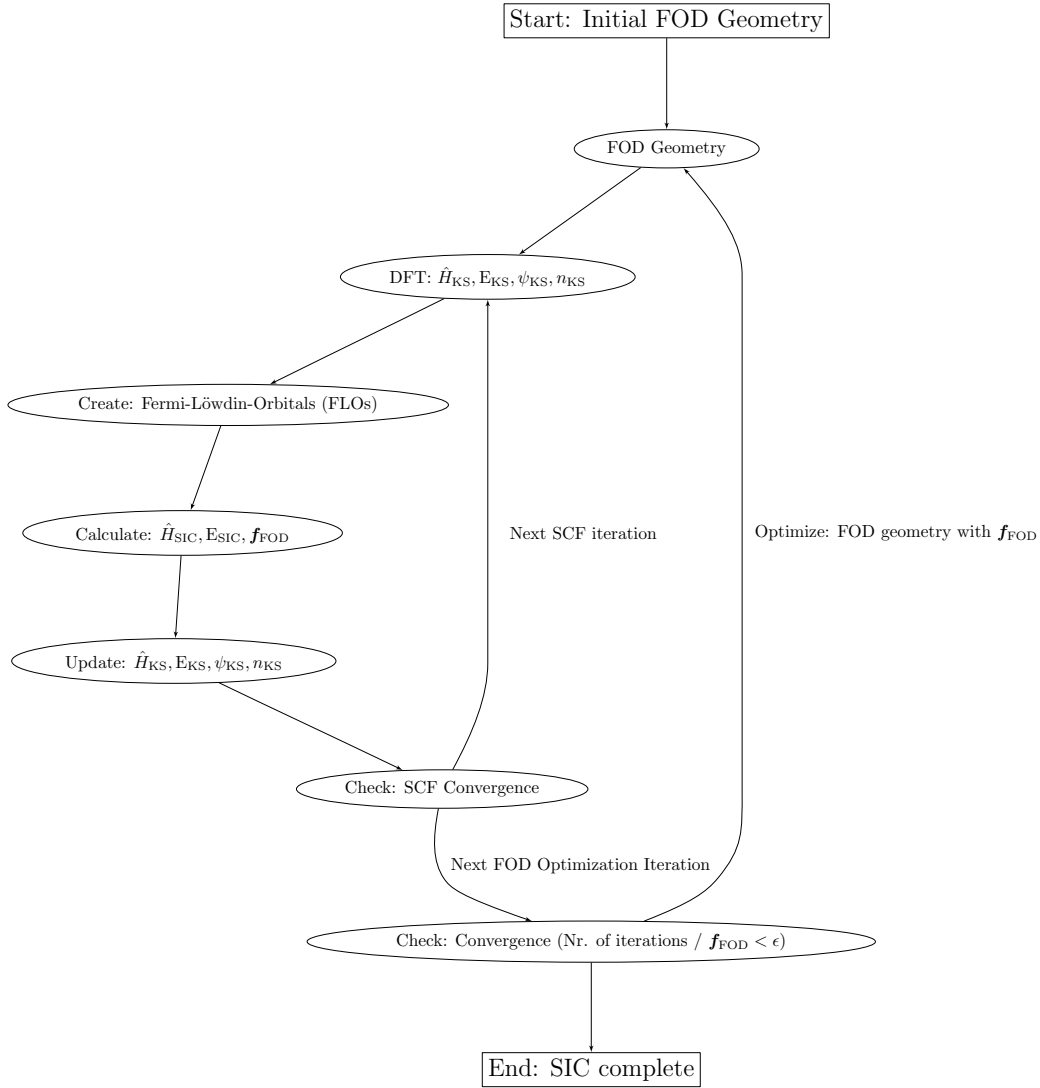


Figure 2: FLO-SIC self-consistent field (scf) flow chart. Initial FODs can be generated with the PyCOM module. The absolute value of the maximal component of the FOD force  $\mathbf{f}_{FOD}$  determines the convergence of the calculation. A FLO-SIC scf calculation is converged when  $\mathbf{f}_{FOD} \leq \epsilon$  with  $\epsilon$  being a numerical threshold (e.g.  $5 \cdot 10^{-3} E_h/a_0$ ).

xyz file (Fig. 3). Having such a file, we can perform standard density functional theory calculations using PySCF. For a PyFLOSIC calculation, we need initial FOD positions in addition to the nuclei positions.

```

2
Nuclei positions
H    0.370700000  +0.000000000  +0.000000000
H   -0.370700000  -0.000000000  -0.000000000

```

Figure 3: Structure of an input file for the H<sub>2</sub> molecule containing nuclei positions only.

### 5.2. Initial FOD generation

Initial descriptors can be generated using the PyCOM module integrated within PyFLOSIC given a nuclei xyz file. A python script for the FOD generation in case of the H<sub>2</sub> molecule is shown in Fig. 4. It relies on the atomic simulation environment, which needs to be available. The script reads atomic positions in standard xyz format. The keywords `charge` and `spin` refer to the charge of the molecule and total spin defined as  $2S$ . The keywords `basis` and `xc` refer to the basis set and exchange-correlation functional used for the DFT calculation.

```

from ase.io import read
from pycom import automatic_guessing

ase_nuclei = read('H2_nuc.xyz')
charge = 0
spin = 0
basis = 'cc-pvqz'
xc = 'LDA,PW'

automatic_guessing(ase_nuclei, charge, spin, basis, xc,
                   method='FB', newton=True, symmetry=False)

```

Figure 4: Python input file for the generation of initial FODs using the PyCOM module.

The result of this initial FOD generation is the PyFLOSIC xyz input file containing nuclei and FOD positions (see Fig. 5). The first line contains an integer value counting the number of all nuclei and FODs within the system. The second line is a comment line, which can include user-defined information. As the next block, each line is listing the nuclei positions in Cartesian coordinates and Ångstrom units. The lines within each block start with a string indicating the chemical symbol followed by three floating values for

the  $(x,y,z)$  positions. The next block introduces the spin-UP FOD positions (marked with symbol X) and the last block contains the spin-DN FOD positions (symbol He). We made the decision to use the X and He symbols for FODs to enable a visualization of FOD positions using standard tools (e.g. Jmol [49], Xcrysden [50], Vesta [51], ase gui [46, 47], etc.). Both chemical symbols are usually represented with a low effective radius in standard visualization tools, thus the FODs are displayed smaller than the nuclei in the system. Due to the ordered block structure the assignment of nuclei positions and FOD positions is always well defined. PyFLOSIC offers the read function *ase2pyscf*, which automatically separates nuclei information from the spin-UP/spin-DN FOD information.

```

4
Nuclei + FOD positions
H    0.370700000 +0.000000000 +0.000000000
H   -0.370700000 -0.000000000 -0.000000000
X   +0.274588624 +0.000000000 +0.000000000
He  -0.274588624 +0.000000000 +0.000000000

```

Figure 5: Structure of an input file for the H<sub>2</sub> molecule. X denotes spin-UP FOD positions, while He refers to spin-DN FOD positions.

### 5.3. Python job file

A basic FLO-SIC calculation within PyFLOSIC can be performed using a simple python script (see Fig. 6). At the first lines starting with *from*, functions needed for the calculation are imported (in this case from ase and PyFLOSIC). The *ase.read* function provides an *ase.object* containing all the nuclei and FOD information (i.e. chemical symbols and positions). The file *H2\_nuc\_fod.xyz* contains the nuclei positions for the H atoms and the initial guess for the descriptor positions, which can be generated using PyCOM. The function *flosic\_optimize* is the call to the PyFLOSIC ase FOD optimizer.

We use many standard variables from PySCF in PyFLOSIC (e.g. *atoms* chemical symbols and positions of the system in PySCF notation, *fod1/fod2* FOD positions (can be read/accessed by the *ase2pyscf* function from an xyz input file), *basis* basis set definition, *xc* exchange-correlation functional, *spin* corresponding to  $2S$ , *charge* total charge, *max\_cycle* maximum number of scf iterations, *conv\_tol* energy threshold for the scf cycle, *grid.level* numerical quality (number of mesh points) of the numerical grid, *verbose* level of

```

from ase.io import read
from ase_pyflosic_optimizer import flosic_optimize

# Load Nuclei+FOD starting geometry.
ase_atoms = read("H2_nuc_fod.xyz")
# The actual pyflosic-scf optimization.
flosic = flosic_optimize('flosic-scf', # mode
                        ase_atoms,
                        0,0, 'LDA,PW',
                        'cc-pvdz', None,
                        opt='FIRE', maxstep=0.1,
                        use_newton=True,
                        use_chk=False,
                        verbose=4)

```

Figure 6: Python input file for a FLO-SIC FOD optimization using the scf mode.

verbosity). The intrinsic variable *mode* selects between one-shot and full scf FLO-SIC calculation. The parameters for geometry optimizers (e.g. *opt* geometry optimizer to be used for the FOD optimization (e.g. 'FIRE', 'CG' or 'LBFGS'), *fmax* maximum value of the absolute FOD force components (in eV/Å), *maxstep* step width for the line search) are set to fit the standard definitions of ase optimizers. Most variables have default values and need not necessarily be given.

## 6. Proof of principles

In this section, we show that the FLO-SIC implementation in PySCF reproduces known exact limits. It is known that DFT shows a qualitatively wrong dissociation behaviour for the  $H_2^+$  molecule, while Perdew-Zunger self-interaction correction (PZ-SIC) gives the correct result [52]. We have calculated the dissociation curve for the prototypical  $H_2^+$  molecule with LDA-, PBE-, and SCAN-FLO-SIC to show that the one-electron self-interaction error is clearly eliminated (see Fig. 7). Hartree-Fock (HF) theory gives the exact solution for this one-electron system, which is reproduced by our PyFLOSIC implementation.

Another test is a comparison of FG-NRLMOL and PyFLOSIC for the G2-1 set (55 small molecules and atoms) [6] using the STO-3G basis set and

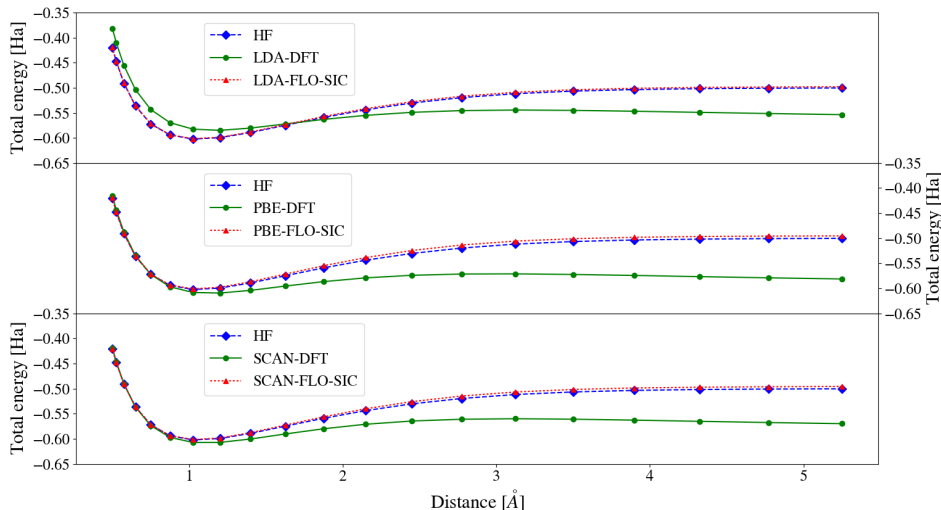


Figure 7: Potential energy of the  $\text{H}_2^+$  molecule. The energy is visualized as a function of distance between the hydrogen atoms. Results are obtained from Hartree-Fock (HF), LDA, PBE, SCAN and the Fermi-Löwdin orbital self-interaction corrected solution on-top of the aforementioned density functionals. For large distances, all semi-local exchange-correlation density functionals deliver a qualitatively wrong behavior. In contrast, FLO-SIC reproduces the exact solution as obtained by Hartree-Fock. Further, FLO-SIC restores the correct dissociation behaviour. This statement holds for FLO-SIC applied to the LDA, the PBE as well as to the SCAN functional.

the LDA exchange-correlation functional (see Fig. 8). The mean absolute error (MAE) for the enthalpies of formation  $\Delta H$  and ionization potentials  $\text{IP} = -\varepsilon_{\text{HOMO}}$  are calculated for this benchmark set.

The MAE is determined by

$$\text{MAE} = \sum_{i=1}^n \frac{|x_{\text{calc},i} - x_{\text{ref},i}|}{n} = \sum_{i=1}^n \frac{|e_i|}{n}, \quad (25)$$

where  $x_{\text{calc},i}$  are the calculated values,  $x_{\text{ref},i}$  the reference values,  $n$  is the total number of values compared and  $e_i$  are the errors. In addition, the mean error (ME) is given by

$$\text{ME} = \sum_{i=1}^n \frac{e_i}{n}, \quad (26)$$

and the mean absolute percentage error (MAPE) is calculated as

$$\text{MAPE} = \frac{100}{n} \sum_{i=1}^n \left| \frac{e_i}{x_{\text{calc},i}} \right|. \quad (27)$$

Standard DFT and FLO-SIC calculations are performed at  $T = 0$  K. We used the G2-1 procedure (for details, see Schwalbe et al. [6]) to obtain the enthalpies of formation, which are defined as the change of the enthalpy of one mole of a substance in the standard state (pressure  $p = 1$  atm and temperature  $T = 298.15$  K) when it is formed from its pure elements under the same conditions. The ionization potential IP is the minimal amount of energy needed to remove the most loosely bound electron (valence electron) from an atom or a molecule. As one can see in Fig. 8, the pure DFT values as well as the FLO-SIC values are in excellent agreement for the reported quantities.

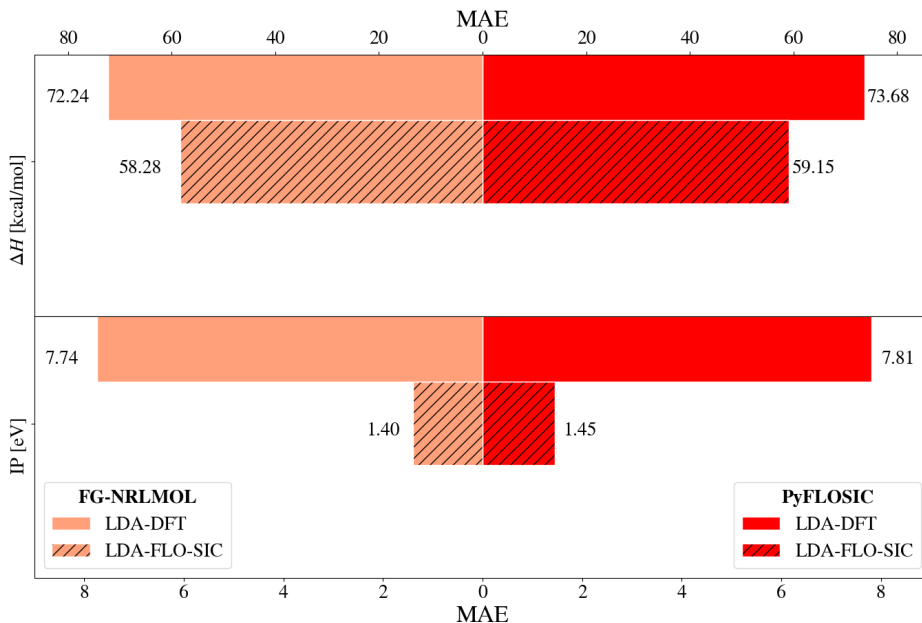


Figure 8: Mean absolute errors (MAE) for the G2-1 set using the STO3G basis set for FLO-SIC applied to the LDA functional.

PySCF offers the possibility to use any standard GTO basis set and pseudopotentials. The Burkatzki-Filippi-Dolg (BFD)-V5Z basis set [53] in combination with corresponding pseudopotentials was used to calculate ionization potentials for some heavy atoms (see Tab. 2). The LDA-FLO-SIC values are in good agreement with experimental values [54]. In addition, FLO-SIC gives a clear improvement compared to the pure LDA values.



Table 2: Ionization potentials  $IP = -\varepsilon_{\text{HOMO}}$  (in eV) for some heavy atoms for LDA and LDA-FLO-SIC compared to experimental values [55]. Numerical parameters for the PyFLOSIC calculation: basis = bfd-v5z (pseudopotential), max cycle = 1000, conv-tol = 1e-5, grid level = 3).

<b>Atom</b>	<b>LDA</b> [eV]	<b>LDA-FLO-SIC</b> [eV]	<b>Exp</b> [55] [eV]
Tl	2.72	5.63	6.11
Pb	3.90	7.00	7.42
Bi	5.22	8.63	7.29
Po	5.07	9.12	8.41
At	6.44	10.55	9.79
Rn	7.87	12.05	10.75
MAE	3.092	0.835	-
ME	-3.092	-0.385	-
MAPE	65.446	8.933	-

## 7. Advanced applications

In the previous section, we showed the numerical agreement between the reference implementation FG-NRLMOL and PyFLOSIC for the G2-1 benchmark set using the small STO-3G basis set. The same benchmark set is used to examine the performance for LDA, PBE and the SCAN functional (see Fig. 9) using the larger density functional optimized (DFO) basis set [48]. The MGGA-SCAN functional is available via the libxc library in our PyFLOSIC implementation. PyFLOSIC results for LDA and PBE are again in good agreement with the FG-NRLMOL values [6] using the DFO basis set. The pure SCAN functional outperforms LDA and PBE, whereas FLO-SIC on top of the SCAN functional performs similar to PBE-FLO-SIC for the enthalpies of formation and the ionization potentials. For ionization potentials and therefore the energy eigenvalues, FLO-SIC improves the accuracy of all three exchange-correlation functionals.

## 8. Conclusion

We implemented the Fermi-Löwdin orbital self-interaction correction as an extension to the PySCF code. This implementation offers the possibility to use FLO-SIC with basis set from the EMSL data base [56, 57], different numerical meshes (e.g. Lebedev-Laikov grids) and any exchange-correlation functional available in the libxc library. Besides this, PyFLOSIC provides an automatic Fermi-orbital descriptor initialization routine - python center of

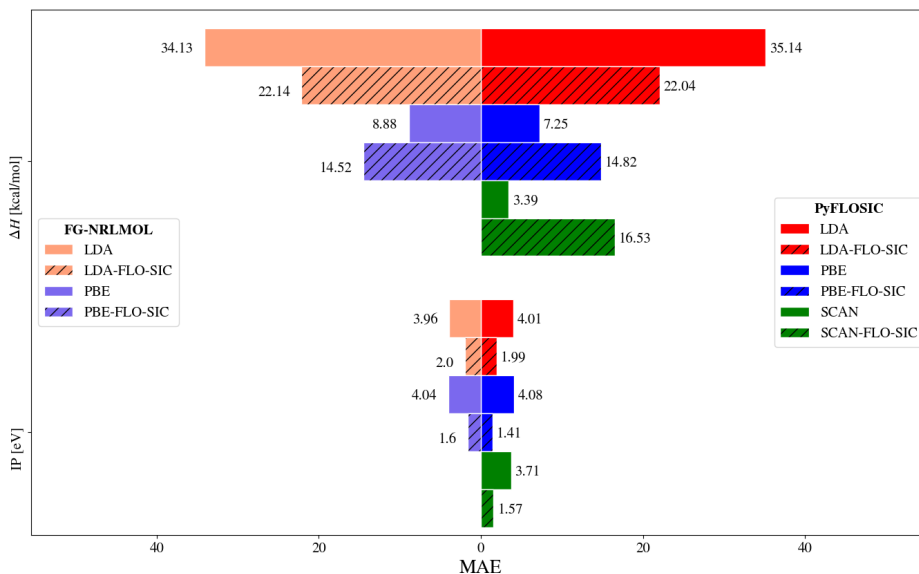


Figure 9: G2-1 errors using the density functional optimized (DFO) basis set for FLO-SIC applied to the LDA, PBE and SCAN functional.

mass (PyCOM) - which increases the usability of FLO-SIC for any user. The implementation of FLO-SIC in PySCF also offers the possibility to benchmark the method against commonly used quantum chemistry methods (e.g. CCSD(T)) using the same basic numerical parameters (e.g. basis sets, evaluation of integrals and numerical mesh).

The LDA, the PBE and the SCAN functional were used to provide proof-of-principles calculations. Further, the performance for the G2-1 benchmark set (see Fig. 9) was analyzed. The thermochemical performance of the functionals confirmed the already well-known observations that only LDA-FLO-SIC decreases the error of the pure functional, while PBE-FLO-SIC and SCAN-FLO-SIC perform worse [6, 52]. It appears that SCAN-FLO-SIC performs slightly worse than PBE-FLO-SIC for the used test case. When investigating ionization potentials and therefore energy eigenvalues, FLO-SIC improves the accuracy of all three exchange-correlation functionals.

Furthermore, due to the modular structure of the PySCF code, PyFLOSIC may be used in combination with solvation models (e.g. COSMO [58, 59]) or it may be extended to work in combination with time-dependent DFT in the future.

## 9. Acknowledgement

Jens Kortus thanks the German Research Foundation (DFG) for financial support of this study KO 1924/9-1. In addition to that, the authors thank the ZIH in Dresden for computational time and support. The authors thank Prof. Susi Lehtola for comments improving the content of the manuscript. K. Treppe is supported by the U.S. Department of Energy, Office of Science, Office of Basic Energy Sciences, as part of the Computational Chemical Sciences Program under Award Number #de-sc0018331.

## References

- [1] P. Hohenberg and W. Kohn. Inhomogeneous Electron Gas. *Phys. Rev.*, 136:B864–B871, 1964.
- [2] W. Kohn and L. J. Sham. Self-Consistent Equations Including Exchange and Correlation Effects. *Phys. Rev.*, 140:A1133–A1138, 1965.
- [3] C. D. Sherrill. Frontiers in electronic structure theory. *J. Chem. Phys.*, 132(11):110902, 2010.
- [4] K. Burke. Perspective on density functional theory. *J. Chem. Phys.*, 136(15):150901, 2012.
- [5] J. P. Perdew, A. Ruzsinszky, L. A. Constantin, J. Sun, and G. I. Csonka. Some fundamental issues in ground-state density functional theory: A guide for the perplexed. *J. Chem. Theory Comput.*, 5(4):902–908, 2009.
- [6] S. Schwalbe, T. Hahn, S. Liebing, K. Treppe, and J. Kortus. Fermi-Löwdin orbital self-interaction corrected density functional theory: Ionization potentials and enthalpies of formation. *J. Comput. Chem.*, 39(29):2463–2471, 2018.
- [7] J. P. Perdew and K. Schmidt. Jacob’s ladder of density functional approximations for the exchange-correlation energy. In *AIP Conference Proceedings*, volume 577, pages 1–20. AIP, 2001.
- [8] J. P. Perdew and Y. Wang. Accurate and simple analytic representation of the electron-gas correlation energy. *Phys. Rev. B*, 45:13244–13249, Jun 1992.

- [9] J. P. Perdew, K. Burke, and M. Ernzerhof. Generalized gradient approximation made simple. *Phys. Rev. Lett.*, 77(18):3865, 1996.
- [10] J. Sun, A. Ruzsinszky, and J. P. Perdew. Strongly Constrained and Appropriately Normed Density Functional. *Phys. Rev. Lett.*, 115:036402, 2015.
- [11] M. R. Pederson. Fermi orbital derivatives in self-interaction corrected density functional theory: Applications to closed shell atoms. *J. Chem. Phys.*, 142(6):064112, 2015.
- [12] M. R. Pederson, A. Ruzsinszky, and J. P. Perdew. Communication: Self-interaction correction with unitary invariance in density functional theory. *J. Chem. Phys.*, 140:121103, 2014.
- [13] Z.-h. Yang, M. R. Pederson, and J. P. Perdew. Full self-consistency in the Fermi-orbital self-interaction correction. *Phys. Rev. A*, 95(5):052505, 2017.
- [14] T. Hahn, S. Liebing, J. Kortus, and M. R. Pederson. Fermi orbital self-interaction corrected electronic structure of molecules beyond local density approximation. *J. Chem. Phys.*, 143(22):224104, 2015.
- [15] T. Hahn, S. Schwalbe, J. Kortus, and M. R. Pederson. Symmetry Breaking within Fermi-Löwdin Orbital Self-Interaction Corrected Density Functional Theory. *J. Chem. Theory Comput.*, 13(12):5823–5828, 2017.
- [16] Q. Sun, T. C. Berkelbach, N. S. Blunt, G. H. Booth, S. Guo, Z. Li, J. Liu, J. D. McClain, E. R. Sayfutyarova, S. Sharma, et al. PySCF: the Python-based simulations of chemistry framework. *Wiley Interdiscip. Rev. Comput. Mol. Sci.*, 8(1):e1340, 2018.
- [17] P. M. W. Gill. Molecular integrals over Gaussian basis functions. In *Adv. Quantum Chem.*, volume 25, pages 141–205. Elsevier, 1994.
- [18] M. R. Pederson, A. Ruzsinszky, and J. P. Perdew. Communication: Self-interaction correction with unitary invariance in density functional theory. *J. Chem. Phys.*, 140(12):121103, 2014.

- [19] M. R. Pederson and T. Baruah. Chapter Eight - Self-Interaction Corrections Within the Fermi-Orbital-Based Formalism. In Ennio Arimondo, Chun C. Lin, and Susanne F. Yelin, editors, *Adv. Atom. Mol. Oop. Phy.*, volume 64, pages 153–180. Academic Press, 2015.
- [20] K. Treppe, S. Schwalbe, T. Hahn, J. Kortus, D.-Y. Kao, Y. Yamamoto, T. Baruah, R. R. Zope, K. P. K. Withanage, J. E. Peralta, and K. A. Jackson. Analytic Atomic Gradients in the Fermi-Löwdin Orbital Self-Interaction Correction. *J. Comput. Chem.*, 40(6):820–825, 2019.
- [21] S. Lehtola and H. Jónsson. Variational, Self-Consistent Implementation of the Perdew-Zunger Self-Interaction Correction with Complex Optimal Orbitals. *J. Chem. Theory Comput.*, 10(12):5324–5337, 2014.
- [22] J. P. Perdew and A. Zunger. Self-interaction correction to density-functional approximations for many-electron systems. *Phys. Rev. B*, 23(10):5048, 1981.
- [23] C. C. J. Roothaan. New developments in molecular orbital theory. *Rev. Mod. Phys.*, 23(2):69, 1951.
- [24] J. A. Pople and R. K. Nesbet. Self-consistent orbitals for radicals. *J. Chem. Phys.*, 22(3):571–572, 1954.
- [25] J. G. Harrison, R. A. Heaton, and C. C. Lin. Self-interaction correction to the local density Hartree-Fock atomic calculations of excited and ground states. *J. Phys. B: Atomic and Mol. Phys.*, 16(12):2079, 1983.
- [26] P.-O. Löwdin. On the non-orthogonality problem connected with the use of atomic wave functions in the theory of molecules and crystals. *J. Chem. Phys.*, 18(3):365–375, 1950.
- [27] J. Kortus and M. R. Pederson. Magnetic and vibrational properties of the uniaxial  $\text{Fe}_{13}\text{O}_8$  cluster. *Phys. Rev. B*, 62(9):5755–5759, 2000.
- [28] M. R. Pederson, K. A. Jackson, and W. E. Pickett. Local-density-approximation-based simulations of hydrocarbon interactions with applications to diamond chemical vapor deposition. *Phys. Rev. B*, 44(8):3891–3899, 1991.

- [29] M. R. Pederson, D. V. Porezag, J. Kortus, and D. C. Patton. Strategies for massively parallel local-orbital-based electronic structure methods. *Phys. Status Solidi (b)*, 217(1):197–218, 2000.
- [30] M. R. Pederson and K. A. Jackson. Pseudoenergies for simulations on metallic systems. *Phys. Rev. B*, 43(9):7312–7315, 1991.
- [31] M. R. Pederson and K. A. Jackson. Variational mesh for quantum-mechanical simulations. *Phys. Rev. B*, 41(11):7453–7461, 1990.
- [32] J. P. Perdew, J. A. Chevary, S. H. Vosko, K. A. Jackson, M. R. Pederson, D. J. Singh, and C. Fiolhais. Atoms, molecules, solids, and surfaces: Applications of the generalized gradient approximation for exchange and correlation. *Phys. Rev. B*, 46(11):6671–6687, 1992.
- [33] D. Porezag. *Development of Ab-Initio and Approximate Density Functional Methods and their Application to Complex Fullerene Systems*. PhD thesis, TU Chemnitz, Fakultät für Naturwissenschaften, 1997. URL <http://archiv.tu-chemnitz.de/pub/1997/0025>.
- [34] S. Lehtola, C. Steigemann, M. J. T. Oliveira, and M. A. L. Marques. Recent developments in libxc-A comprehensive library of functionals for density functional theory. *SoftwareX*, 7:1–5, 2018.
- [35] L. Fiedler. Master thesis: Implementation and reassessment of the Fermi-Löwdin orbital self-interaction correction for LDA, GGA and mGGA functionals, 2018.
- [36] Q. Sun. Libcint: An efficient general integral library for Gaussian basis functions. *J. Comput. Chem.*, 36(22):1664–1671, 2015.
- [37] J. Lehtola, M. Hakala, A. Sakko, and K. Hämäläinen. ERKALE - A flexible program package for X-ray properties of atoms and molecules. *J. Comput. Chem.*, 33(18):1572–1585, 2012.
- [38] S. Lehtola and H. Jónsson. Unitary optimization of localized molecular orbitals. *J. Chem. Theory Comput.*, 9(12):5365–5372, 2013.
- [39] S. Schwalbe, K. Trepte, L. Fiedler, A. I. Johnson, J. Kraus, T. Hahn, J. E. Peralta, K. A. Jackson, and J. Kortus. Interpretation and automatic generation of Fermi-orbital descriptors. *submitted to J. Comput. Chem.*, 2019.

- [40] C. G. Broyden. The convergence of a class of double-rank minimization algorithms 1. General considerations. *IMA J. Appl. Math.*, 6(1):76–90, 1970.
- [41] R. Fletcher. A new approach to variable metric algorithms. *Comput. J.*, 13(3):317–322, 1970.
- [42] D. Goldfarb. A family of variable-metric methods derived by variational means. *Math. Comput.*, 24(109):23–26, 1970.
- [43] D. F. Shanno. Conditioning of quasi-Newton methods for function minimization. *Math. Comput.*, 24(111):647–656, 1970.
- [44] J. Nocedal. Updating quasi-Newton matrices with limited storage. *Math. Comput.*, 35(151):773–782, 1980.
- [45] E. Bitzek, P. Koskinen, F. Gähler, M. Moseler, and P. Gumbsch. Structural Relaxation Made Simple. *Phys. Rev. Lett.*, 97:170201, 2006.
- [46] A. H. Larsen, J. J. Mortensen, J. Blomqvist, I. E. Castelli, R. Christensen, M. Dulak, J. Friis, M. N. Groves, B. Hammer, C. Hargus, et al. The atomic simulation environment - a Python library for working with atoms. *J. Phys. Condens. Matter*, 29(27):273002, 2017.
- [47] Atomic Simulation Environment. <https://wiki.fysik.dtu.dk/ase/>, 2018.
- [48] D. Porezag and M. R. Pederson. Optimization of Gaussian basis sets for density-functional calculations. *Phys. Rev. A*, 60(4):2840, 1999.
- [49] R. M. Hanson. Jmol—a paradigm shift in crystallographic visualization. *J. Appl. Crystallogr.*, 43(5):1250–1260, 2010.
- [50] A. Kokalj. Xcrysden - a new program for displaying crystalline structures and electron densities. *J. Mol. Graph. Model.*, 17(3-4):176–179, 1999.
- [51] K. Momma and F. Izumi. Vesta: a three-dimensional visualization system for electronic and structural analysis. *J. Appl. Crystallogr.*, 41(3): 653–658, 2008.

- [52] C. Shahi, P. Bhattarai, K. Wagle, B. Santra, S. Schwalbe, T. Hahn, J. Kortus, K. A. Jackson, J. E. Peralta, K. Treppe, S. Lehtola, N. K. Nepal, H. Myneni, B. Neupane, S. Adhikari, A. Ruzsinszky, Y. Yamamoto, T. Baruah, R. R. Zope, and J. P. Perdew. Stretched or noded orbital densities and self-interaction correction in density functional theory. *J. Chem. Phys.*, 150(17):174102, 2019.
- [53] M. Burkatzki, C. Filippi, and M. Dolg. Energy-consistent pseudopotentials for quantum Monte Carlo calculations. *J. Chem. Phys.*, 126(23):234105, 2007.
- [54] A. Kramida, Yu. Ralchenko, J. Reader, and NIST ASD Team. NIST Atomic Spectra Database (ver. 5.5.6), [Online]. Available: <https://physics.nist.gov/asd> [2018, May 24]. National Institute of Standards and Technology, Gaithersburg, MD., 2018.
- [55] R. D. Johnson. *NIST Computational Chemistry Comparison and Benchmark Database*. NIST Standard Reference Database Number 101, 18–10–2016. URL <http://cccbdb.nist.gov/>.
- [56] D. Feller. The role of databases in support of computational chemistry calculations. *J. Comput. Chem.*, 17(13):1571–1586, 1996.
- [57] K. L. Schuchardt, B. T. Didier, T. Elsethagen, L. Sun, V. Gurumoorthi, J. Chase, J. Li, and T. L. Windus. Basis set exchange: a community database for computational sciences. *J. Chem. Inf. Model.*, 47(3):1045–1052, 2007.
- [58] A. Klamt and G. J. Schüürmann. Cosmo: a new approach to dielectric screening in solvents with explicit expressions for the screening energy and its gradient. *J. Chem. Soc., Perkin Trans. 2*, (5):799–805, 1993.
- [59] T. N. Truong and E. V. Stefanovich. A new method for incorporating solvent effect into the classical, ab initio molecular orbital and density functional theory frameworks for arbitrary shape cavity. *Chem. Phys. Lett.*, 240(4):253–260, 1995.